UNIVERSITY OF CALIFORNIA SAN DIEGO

Small Disturbance, Long Term Voltage Stabilization on a Distribution Feeder in Kathmandu, Nepal

A thesis submitted in partial satisfaction of the requirements for the degree Master of Science

in

Engineering Sciences (Mechanical Engineering)

by

Nikhar Jung Abbas

Committee in charge:

Professor Jan Kleissl, Chair
Professor Carlos Coimbra
Professor Raymond de Callafon

2016

The Thesis of Nikhar Jung Abbas is approved, and it is acceptable in quality and form for publication on microfilm and electronically.

Chair

University of California, San Diego

2016

Table of Contents

List of Figures

List of Tables

ABSTRACT OF THE THESIS

Small Disturbance, Long Term Voltage Stabilization on a Distribution Feeder in Kathmandu, Nepal

by

Nikhar Jung Abbas

Master of Science in Engineering Sciences (Mechanical and Aerospace Engineering)

University of California, San Diego, 2016

Professor Jan Kleissl, Chair

Penetration of solar photovoltaic (PV) generation into power distribution grids is happening around the globe. Recent research has indicated that the coordination of these technologies' functions with the existing grid infrastructure can help mitigate the adverse effects on voltage stability that has been observed with decentralized generation. The volt-var control functionality of smart inverters is often considered for mitigation of both short and long term, small disturbances to voltage. In many studies, smart inverter volt-var control functionality is primarily considered to mitigate overvoltage and reverse power flow. This research demonstrates the use of smart inverter volt-var control to mitigate long term, highly variable voltage deviations from the nominal voltage on a distribution feeder in Kathmandu, Nepal. The work considers data collected from an existing, grid-tied, PV plus battery system to show the feasibility of voltage stabilization in a region with an inconsistent power supply from the local utility.

1 Introduction

1.1 Voltage Stability

The stability of power systems has been under review since the beginning of the 20th century [1]. This review has lead the understanding of three main classifications of power system stability: Rotor Angle Stability, Frequency Stability, and Voltage Stability [2][3]. As power systems have evolved over time, stability has become a greater concern than ever before. An increasing number of feeder interconnections, new technological developments, control solutions, dynamic and high stress loads, and the introduction of distributed energy resources have changed distribution feeder topologies drastically [4].

While the power distribution system of today is more complicated than ever, recent developments in technology offer the possibility to mitigate the new and old factors causing power system instabilities [4]. As discussed in [5], the terminal voltage of a feeder is susceptible to drop due to transmission of large amounts of power over long electrical distances. By analyzing and adjusting the power factor, these voltage drops can be mitigated to some extent. This is sometimes implemented by the introduction of capacitor banks which help to move the power factor from lagging to leading. New, smart inverter volt-var control techniques have introduced a more adaptive method to adjusting the power factor by their ability to act as both an inductive and capacitative load[6]. This research focuses smart inverter volt-var control for stabilizing small-disturbance, long term voltage instability, as defined in [3].

1.2 RIDS Nepal Case Study

RIDS-Nepal is a non-governmental agency focused in rural, holistic, community development in Nepal. Though operating primarily in the extremely remote Himalaya regions of Nepal, the organization has an office located in the country's capital, Kathmandu. This site contains, a 1.11 kWp PV system, 275 Ah battery bank, and two inverters rated at a combined 3.6 kVA, amongst numerous monitors and sensors. The system is located far from it's distribution feeder's transformer, and operates in both grid tied and islanded modes. Data is collected and transfered to an online server every ten minutes. This data is then posted in one hour intervals on the group's website, pvnepal.com for public educational usage. The scope of this data ranges to nearly 50 different fields. These fields include environmental data such humidity and solar irradiation, temperatures of the

air and of PV modules, and electrical characteristics such as voltage, current, and power factor at numerous nodes in the system. The primary goal of this research is to and assess viability of smart inverter volt-var voltage control on a highly variable power distribution feeder.

1.3 Project Goals

In order to adequately address and assess the voltage stability issue of the feeder, three specific aims are defined:

1. To reconstruct the local topography of the distribution feeder and maintain consistency with data collected from the RIDS-Nepal office.
2. To optimize the volt-var control curve for the distribution feeder model.
3. To characterize the stability offered by the control curve through distribution system power flow simulations and analysis.

The open source distribution system simulation software produced by EPRI, OpenDSS, was used to perform the stability analysis [7]. These simulations were used to show the reconstructed feeder and the implemented voltage stabilization actions. After the distribution feeder model was defined in OpenDSS, simulation results were used to define an optimal volt-var control curve. This curve defines a reactive power(Q) output from the inverters that modifies the voltage to a satisfy a defined stability criteria. The OpenDSS software package is designed for frequency domain analysis, and thus is not typically used for time domain, transient, analysis. The control implementation methods established in [6] was used to conduct daily simulations with implemented control action. A step ahead predictor was used to define the successive time step's Var output from the inverters. The performance of this controller was characterized by its ability to stabilize the voltage.

2 Motivation and Methods

In order to successfully complete the established goals of this project, the research follows 5 steps of action:

1. Reconstruction of the distribution feeder.
2. Formulation of a state predictor for the distribution feeder.
3. Development of a volt-var control scheme.
4. OpenDSS power flow simulations.
5. Analysis and Validation of results to quantify performance.

The motivation and methodologies by which these steps are implement is discussed in a greater detail in the subsequent sections.

2.1 Feeder Reconstruction

Although the data collected from the RIDS-Nepal site is extremely extensive, the conditions of the distribution feeder that the site is connected to are not well known. Fortunately, for the purpose of local voltage stability analysis, detailed knowledge of the entire feeder is not necessary. Rather, it is important that the location of the site and a few surrounding nodes are well modeled. For this reason, we started with a simple feeder line of a format seen in Figure 1. In this simplification, it clear that we do not need to model the feeder outside of the box seen in the figure, as long as input conditions to the model produce modeled voltages within the site that are consistent with the measured voltages.

The next important aspect to the reconstruction and modeling of the power distribution system is the RIDS-Nepal Office site itself. This is the most complex distributed energy system in the region, and was the first of its kind to offer the possibility of feeding power into the existing distribution system [8]. Figure 2 is a detailed schematic diagram showing the numerous power electronic devices, sensors and monitors, and their circuitry within the RIDS-Nepal office site. At the PV and Battery system locations, our elements of concern are the inverters, as they will be our reactive power sources. Combining these two simplified systems seen in Figures 1 and 2, we finally arrive at the simple circuit diagram seen in figure 3. This circuit diagram represents the model which is constructed within the OpenDSS framework for power flow simulation. The last step in completing the reconstruction of the distribution feeder is to characterize critical nodes of this

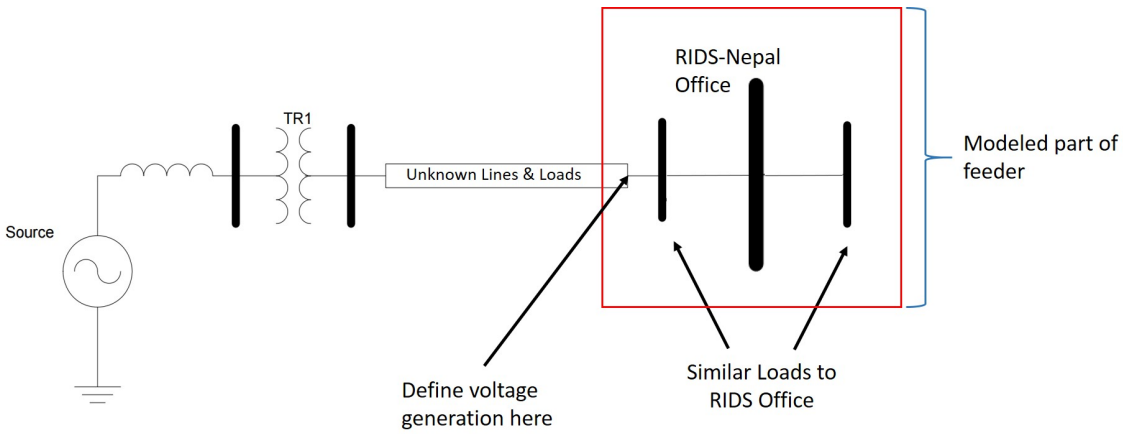

Figure 1: Simplified distribution feeder line considered for the purposes of localized voltage analysis near the RIDS-Nepal office. For the purposes of this study,a detailed model of the system components outside of the red box is not necessary, as long as the feeder conditions at a boundary upstream from the node in question are well defined.

system to create the voltage conditions seen in the collected data.

Though there are no direct measurements of the distribution feeder voltage, the inverter connected to the battery system is a grid-tied 3 way inverter. At any point in time, this inverter is drawing power to or from a DC connection to the battery bank, an AC connection to the grid, or not at all. The inverter voltage is measured only when there is an AC connection between the power grid and the RIDS-Nepal system. This relation is seen in Figure 4. If the system has islanded itself from the grid or is using the battery, there is no measurement of voltage seen from this inverter. With this known, we can defined feeder voltage $V_f = V_{xtend}$ when the voltage measurement is identical at all nodes of the system, or when equation 1 holds.

$$Vuser = Vsma = Vxtend \tag{1}$$

With:

$Vuser \triangleq$ User voltage

$Vsma \triangleq$ PV connected SMA inverter AC voltage

$Vxtend \triangleq$ Grid and battery connected Studer Xtender inverter AC voltage

When equation 1 does not hold, we must fill the missing datapoints with reasonable data. Because the purpose of this study is to establish the usage of smart inverter volt-var control on a feeder of this variability, preserving the exact values of the voltage on feeder at a given point in time is less important than preserving the variability of the feeder voltage over time. Three methods are

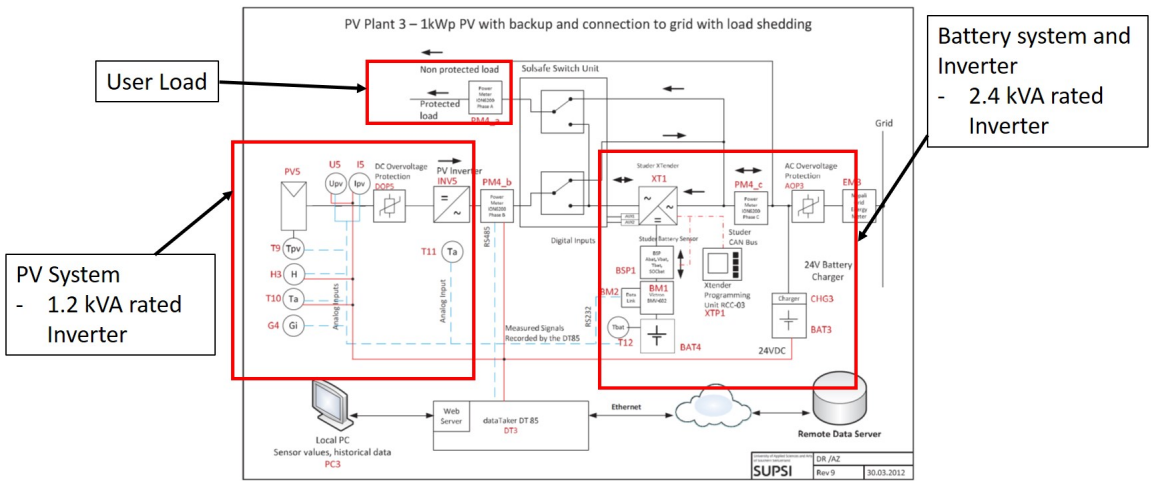

Figure 2: RIDS Nepal schematic of the power distribution system at the office's site it Kathmandu, Nepal. The schematic is sectioned into three primary areas of power consumption or generation: The PV system, battery system, and user load. These sections are highlighted by the red boxes in the diagram.

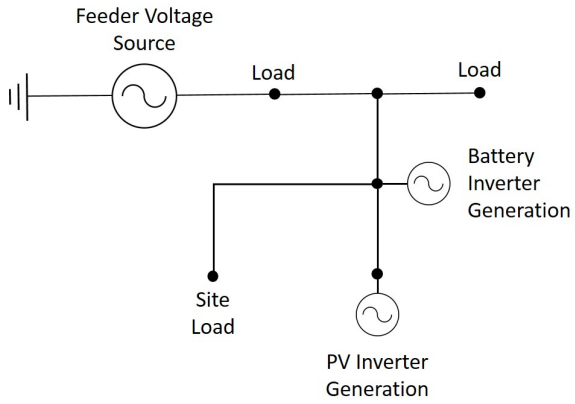

Figure 3: Modeled feeder diagram showing the simple distribution feeder created in OpenDSS for the purpose of this work.

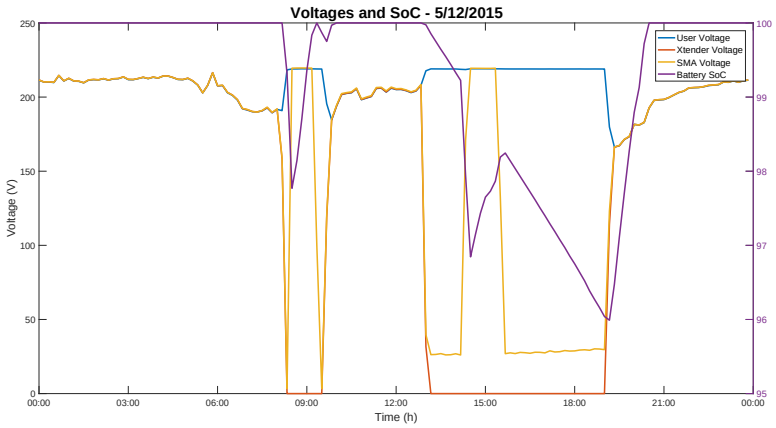

Figure 4: 5/12/2015 Voltages and Soc at RIDS-Nepal Office. It is noted that when the voltage of the Xtender inverter is zero, the system is islanded from the grid. This is assumed because the battery is either discharging, or charging while the PV inverter is supplying power to both the site and battery.

used to fill the missing data. First, if data from the same time during a different year is available, this data is duplicated for the current time being considered. Otherwise, for data gaps of less than three time steps, a simple linear interpolation between the two known voltages is done. For data gaps of greater than three time steps, a line is interpolated from the two known voltages with an added randomness that preserves the the variability of the system. It should be noted that, were smart inverter control to be used in this system, this filled data would never be of importance as the control is general implemented in continuous time [6]. At most times for which Equation 1 does not hold, it is because the system has islanded and is stable at a nominal voltages. For the purpose of consistency in the variability throughout each day, the system voltage was considered as the reconstructed feeder voltage as defined in this section. This, in effect, increases the complexity of the problem, but provides for consistency in data from simulation outputs.

The user load should be met as the data indicates, so we simply define the power at every point in time for the user's load as the kW measured. Because our definition of the voltage source from the power grid was designed without separating the voltage change as a result of the power output from the two inverters, we assume that the power output from the distribution feeder generation then encompasses any real power output that may have been from the inverters during data collection. Thus, we nominally set the inverter kW output to zero in order to preserve the voltage conditions of the site. Finally, we leave the inverter reactive power (Var) output to be determined as the simulation runs. Table 1 displays the constraints applied to the distribution system simulation's

elements.

Table 1: Constraints on Power Flow Simulations

Element	Parameter	Value
Vsource	Voltage	Feeder voltage as found
Lines	Resistance	0.530208 Ω/km
	Impedance	0.281345 Ω/km
	Capacitance	2.12257 nF/km
	Phases	1
Loads	Active Power	Random load (kW) similar to measured PV-Nepal load
Cite Load	Active Power	Measured Load
Inverters	Reactive Power	Optimal kVAr calculated
	Active Power	0

2.2 Predictor Formulation

In order to accurately define the desired Var output from the inverters, a predictor was implemented to predict what the voltage would be without any volt-var control. Equations 2-6 show the two steps of the predictor, a measurement update and a time update.

Measurement Update:

$$e(t) = \bar{v}(t) - v(t) \tag{2}$$

$$\hat{v}(t) = \hat{v}(t) - e(t) \tag{3}$$

$$\hat{v}(t+1) = \hat{v}(t) + [\hat{v}(t) - \hat{v}(t-1)] \tag{4}$$

Time Update:

$$\hat{v}(t-1) = \hat{v}(t) \tag{5}$$

$$\hat{v}(t) = \hat{v}(t+1) \tag{6}$$

Equation 2 is simply an error between the expected voltage at the site after control, $\bar{v}(t)$, and the actual measured voltage after the power flows has converged, $v(t)$. This error was used to modify the prediction from the preceding time step to be a corrected value $\hat{v}(t)$ in Equation 3 to increase the accuracy of the next prediction. Equation 4 is the calculation of the predicted voltage without control. This was done by assuming linearity between the voltage at the current and previous time steps. Equations 5 and 6 update the measurements to the next time step.

2.3 Optimal Volt-Var Development

The methods by which an optimal volt-var curve should be found have not been defined explicitly. This is namely due to the variable nature of the curves, their dependency on the systems on which they are implemented, and changing definitions of the optimality condition. The work presented in [9] does discuss the uses of optimal volt-var curves and provides a general case shown in Figure 5.

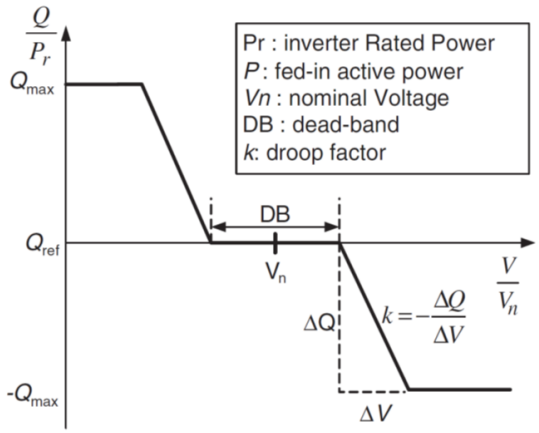

Figure 5: Standard volt-var curve showing the typical aspects of a volt-var curve used for smart inverter control [9].

This piecewise function defines an output reactive power (Q) based on the measured voltage in order to change the node voltage to a desired value. In practice and in research, this $Vdes$ is defined as the nominal feeder voltage, and thus the voltage setpoint of the volt-var is 1pu. This definition is primarily a consequence of the scope of research or location of implementation of the smart inverter. The distribution systems where volt-var control curves are better understood generally consider a deviation greater than $\pm.05pu$ to $\pm.1pu$ to be fatal. On the distribution in question, voltage deviations of over $\pm.2pu$ (generally under voltage) are seen regularly.

In addition to the voltage setpoint, a voltage dead-band is often considered for the optimal volt-var curve. This relaxes the condition on the optimal voltage, but offers a more robust scheme for systems of high solar penetration and distribution of smart inverters with Var output. For this study, we consider a localized inverter dispatch and have no need to relax this optimality condition [9]. Smart inverter control is generally implemented in two modes, supervisory and local. Supervisory control implements control via communications with other grid-connected elements and aims to offer

broader network stability, while local voltage control focuses on stabilizing the inverter connection as well as possible. The latter of these control modes is better supported by a volt-var curve defined without a dead-band.

The final aspect of the defined volt-var curve is the slope of the dispatch line, often referred to as a droop factor, k. Changes in this optimal droop factor are caused by the penetration of power from the inverters. We define this penetration as a unit-less percentage comparing the maximum operating power of the inverters to the maximum load of the feeder.

$$\%penetration = \frac{kVAp_{inverters}}{kVAp_{load}} \tag{7}$$

It should be noted that the due to the relatively small PV penetration power of the installed inverters, there is not enough power to significantly modify the voltage of the feeder. For the purpose of this analysis, the %penetration will be increased by approximately one order of magnitude, simulating a larger PV system at the distribution site, and nothing more. Equation 8 describes a voltage at neighboring nodes for a linear model defined with two loads at each node in short distribution feeder [10].

$$v_{i+1} = \frac{v_i + R_{i,i+1}P_i + X_{i,i+1}Q_i}{v_i^2} \tag{8}$$

With:

$$v_{i+1} = v_{user}$$

$$v_i = v_{inv}, \quad v_{inv} = v_{sma} = v_{xtend}$$

$$R_{i,i+1} = \text{Line resistance between nodes}$$

$$X_{i,i+1} = \text{Line impedance between nodes}$$

$$P_i, Q_i = P_{inv}, Q_{inv}$$

This equation was introduced to present a mathematical representations of the feeder and propose optimizations of a volt-var curve as calculated by this representations. The outcome of this optimization was used to aid in defining a final voltage setpoint and deadband for our implemented

volt-var curve by the minimization function:

$$\min_{V_{set},DB} \left[var(V),\ \%Violations\right] \tag{9}$$

Subject to:

$$v_{set} \in [v_{min} : v_{max}]$$

$$DB \in [0 : DB_{max}]$$

Where:

$$V = \{v_{user}(1), ..., v_{user}(t-1), v_{user}(t)\}$$

$$\%Violations = \frac{|\{abs(v_{user} - v_{set}) > tol\}|}{t}$$

The minimization in Equation 9 was done for all possible values of v_{set} and DB. The applied volt-var curve on the mathematical formulation of the problem that minimized $var(V)$ and $\%Violations$ defined a proposed optimal setpoint and deadband. The following iterative process was then used to find the optimal volt-var curve for the constructed feeder model:

1. An average operational power is defined
2. A set of voltages $[V_{min} : V_{max}]$ is established as encompassing operational voltages of the system
3. The range of Var output of the inverters $[-Q_{max} : Q_{max}]$ is established, where Q_{max} is the maximum rated Var output of the inverters.
4. Inverter voltage defined as $v_{inv} \in [v_{min}, v_{max}]$
5. Inverter Var defined as $Q_{inv} \in [-Q_{max}, Q_{max}]$
6. The mathematical model or power flow simulation is solved(converged) to find the voltage at the user.
7. Steps 5 and 6 are repeated for all $Q_{inv} \in [-Q_{max}, Q_{max}]$ until $v_{user} = v_{set}$ where V_{des} is the desired user voltage.
8. Q_{inv}, v_{inv} stored
9. Steps 4-8 repeated for all V_{inv}. For iterations when $V_{user} \neq V_{des}$ ever, $\pm Q_{max}$, V_{inv} is stored.

As a result of this process, the optimal inverter reactive powers that resulted in user voltages at the desired nominal value were found and an optimal volt-var curve was created. In addition, every Q_{inv} and V_{inv} were stored in step 7, so a lookup table could be formulated. Through this lookup table, it was possible to quickly determine a $V_{expected} \approx V_{user}$ for any Q_{inv} and V_{inv}. This was useful to maintain performance of the predictor while shortening the time necessary for power

flow simulations.

2.4 Power Flow Simulation

For the purpose of the power flow analysis portion of this work, the distribution system simulation software, OpenDSS, is driven through a a MATLAB communication(com) interface. This makes rapid data processing and analysis possible for the power flow simulations. Because OpenDSS solves a frequency domain problem, daily simulations were done incrementally, while implementing control actions and outcomes in a discrete time analysis. The proposed power flow simulation steps in [6] that this work duplicates, along with the implementation methods and interpretation of these steps, are as follows:

1. Initialize node voltages
    - Define the feeder conditions as defined in section 2.1.
2. Solve for node voltages
3. Repeat 2 and 3 until power flow converges
    - Note: steps 2 and3 are simply the function of OpenDSS and are never modified in the scope of this work
4. Sample control element inputs
    - Measure voltage at site in order to determine the necessary VAr output of the inverter based on the defined Volt-VAr curve.
5. Take control actions
    - Apply predicted VAr to attempt to drive user voltage to nominal point.
6. Repeate 2 through 6 until no more control actions for defined time

These steps above are implemented using Equations 2:6 from the predictor formulation, and Equations 10 and 11 which represent the volt-var curve implementation and OpenDSS power flow simulation, respectively. In this representation, $\bar{q}(t)$ is reactive power calculated to stabilize $\hat{v}(t)$, $\bar{v}(t)$ is the expected resultant voltage of the stabilization from $\bar{q}(t)$. Equation 11 represents the OpenDSS solution, where the only input changed during the simulation is $\bar{q}(t)$, and the output of importance is $v(t)$.

Predictor Measurement Update:

$$e(t) = \bar{v}(t) - v(t) \tag{2}$$

$$\hat{v}(t) = \hat{v}(t) - e(t) \tag{3}$$

$$\hat{v}(t+1) = \hat{v}(t) + [\hat{v}(t) - \hat{v}(t-1)] \tag{4}$$

Predictor Time Update:

$$\hat{v}(t-1) = \hat{v}(t) \tag{5}$$

$$\hat{v}(t) = \hat{v}(t+1) \tag{6}$$

Volt-Var Curve Calculations:

$$[\bar{q}(t), \bar{v}(t)] = H(\hat{v}(t)) \tag{10}$$

OpenDSS Power Flow Simulation:

$$v(t) = G(\bar{q}(t)) \tag{11}$$

2.5 Validation

The control system was validated using two simple measures. First, the variance was used to asses overall voltage stability. Second, the time during which the voltage was within a defined tolerance was used to characterize how well the voltage was controlled. This made it possible to asses both the quality of the stabilization algorithm, along with how well it performed.

3 Data and Results

For the purposes of consistency, most results presented are from data collected on May 20th, 2015. This day was chosen simply because the RIDS-Nepal office does not island throughout this day, so Equation 1 holds 6.

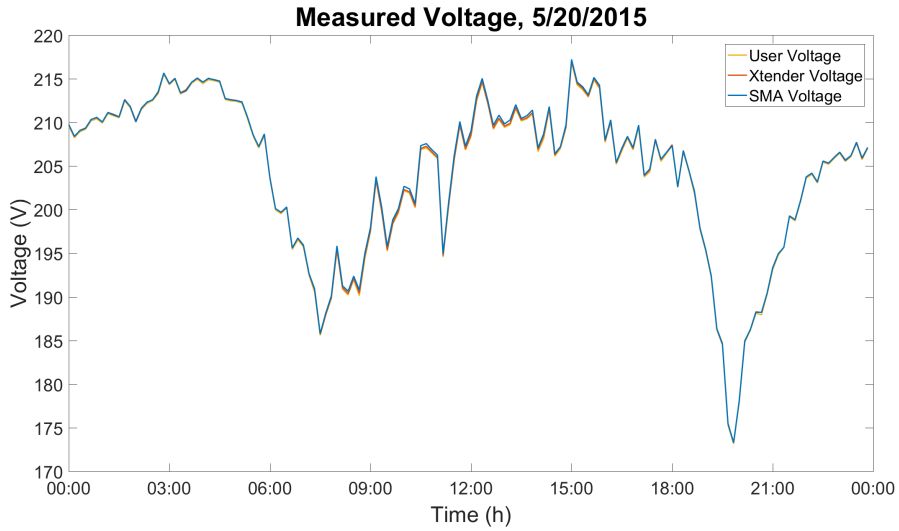

Figure 6: All measured voltages on 5/20/2015 from each of the inverters and the user. It is seen that all voltages are equal, so Equation 1 holds.

3.1 Feeder Reconstruction

In order to consider how well we have reconstructed the feeder, the voltages from the actual and modeled feeder are compared in Figure 9. The reconstructed feeder voltage is also presented in Figure 10 for the days of 5/12/2015 and 5/13/2015.

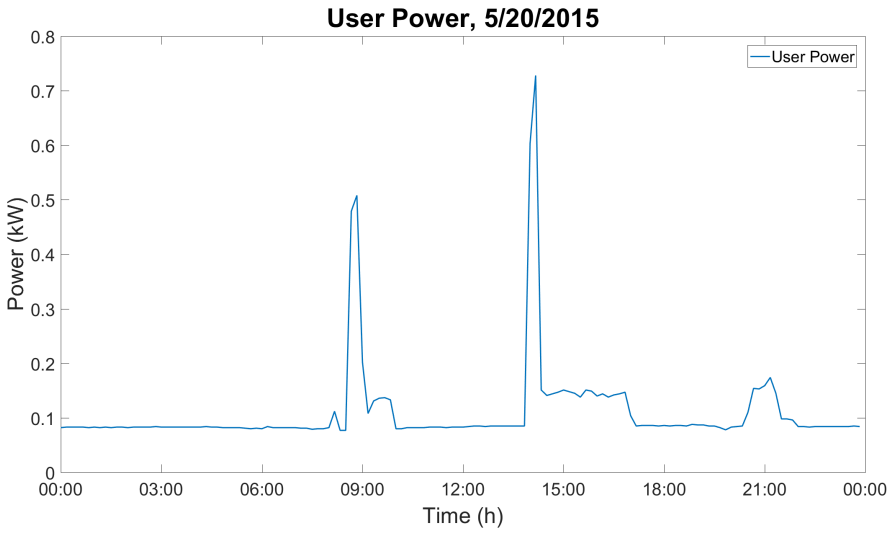

Figure 7: User power consumption on 5/20/2015 in kW. Typical residential usage is seen on this day, with a peak in the morning and a peak in the evening.

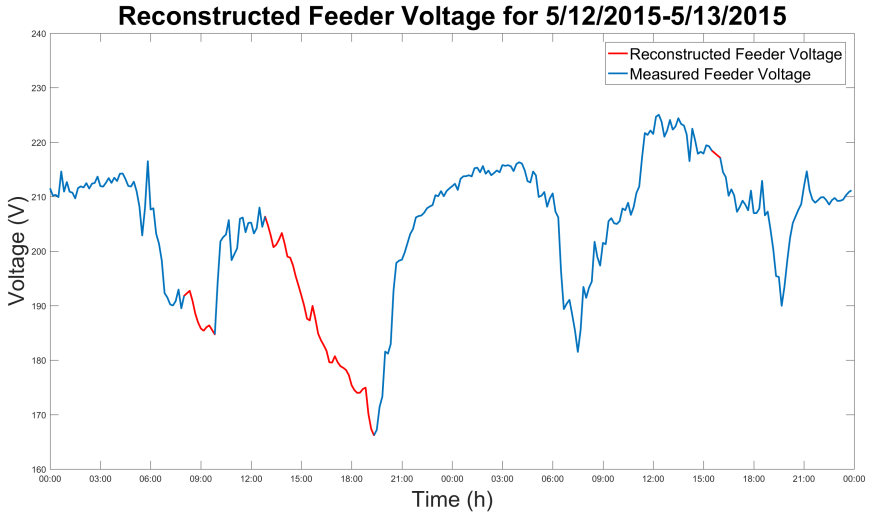

Figure 10: Reconstructed feeder voltage for the days of 5/12/2015-5/13/2015. Though not necessary for most aspects of this analysis, reasonable reconstruction of the feeder voltage would be necessary for longer term analysis of the collected data.

3.2 Predictor

In order to consider the performance of our predictor algorithm, the predicted voltage without any volt-var applied is compared to the actual voltage in Figure 11.

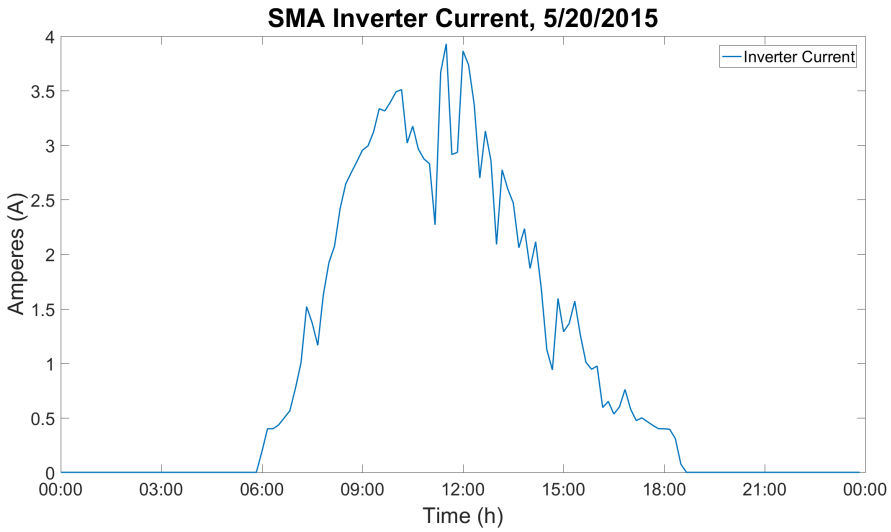

Figure 8: PV inverter current on 5/20/2015 in kW. The SMA inverter is the inverter connected to PV system. The output current from this inverter is expected to follow a similar trend to that of typical solar irradiance.

3.3 Optimal Volt-Var

Both mathematical and model based formulations of the optimal volt-var curve are found. The optimality conditions found from mathematical formulation defined by Equation 8 are used to define the setpoint and deadband of the OpenDSS model-based volt-var curve. The surface plots that represent the minimization of variance and minimization of voltage violations are seen for the mathematical formulation of this problem in 12 and 13. The result of applying these conditions to define a volt-var curve are seen for the mathematical and actual model in Figures 14, and 13, respectively.

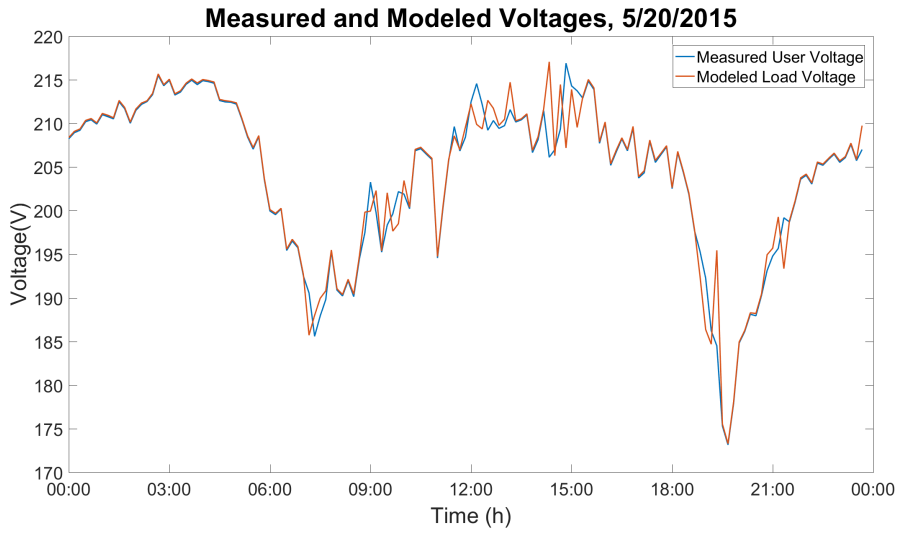

Figure 9: Actual and Modeled Voltages at the user are shown. The variability is preserved, and the voltages levels follow similar trends.

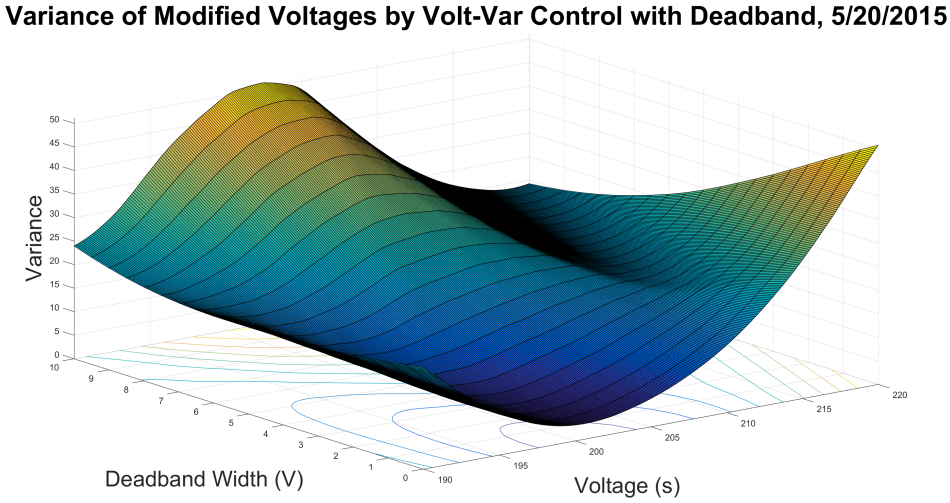

Figure 12: Surface plot of variance from mathematical model given a specified voltage setpoint and tolerance. Equation 8 was solved for voltages defined for 5/20/2015 and a stabilizing reactive power. The variance of the voltages throughout the day is shown here.

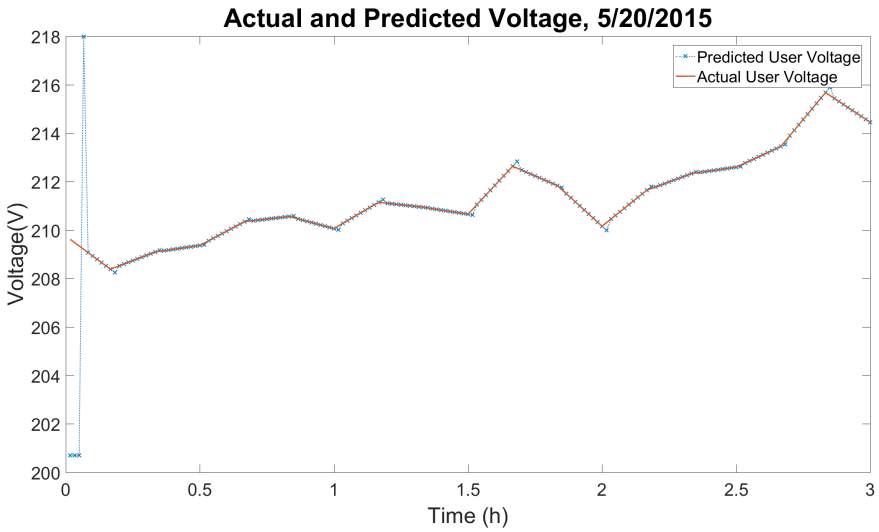

Figure 11: Predictor performance is seen here. We note that since the predictor assumes linearity from the previous time-step to predicted the next time step, and then corrects for any errors.

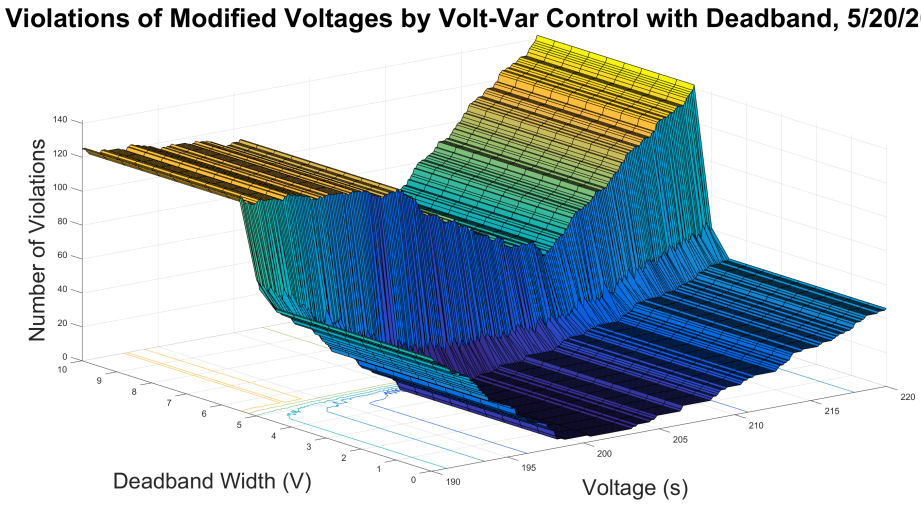

Figure 13: Surface plot of voltage violations from mathematical model given a specified voltage setpoint and tolerance. A tolerance of 5 volts was given, which explains the extreme increase of violations after the 5 Volt deadband width, as the volt-var curve is no longer defining a reactive power to give a voltage that we consider optimal.

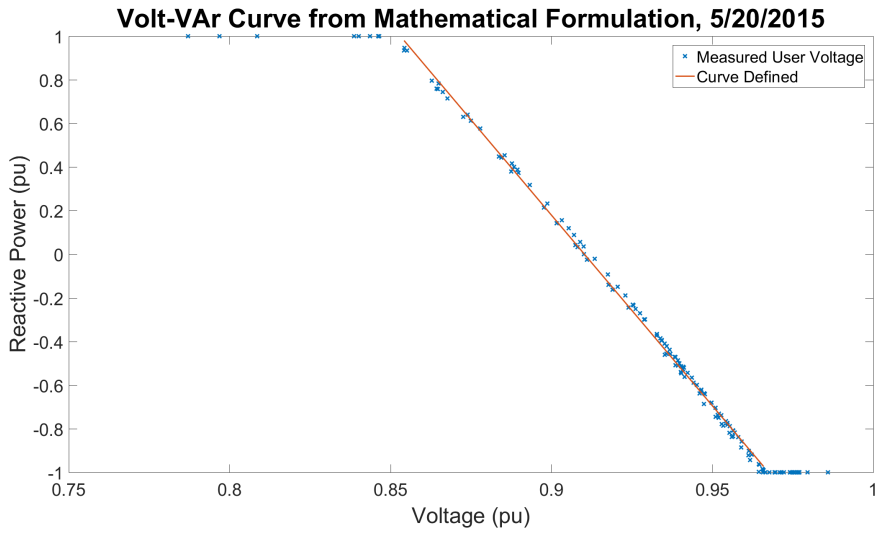

Figure 14: Volt-Var curve as defined by the mathematical model, given the minimum variance optimality conditions as seen in 2. The slope of the linear fit to the data is the droop factor of this curve.

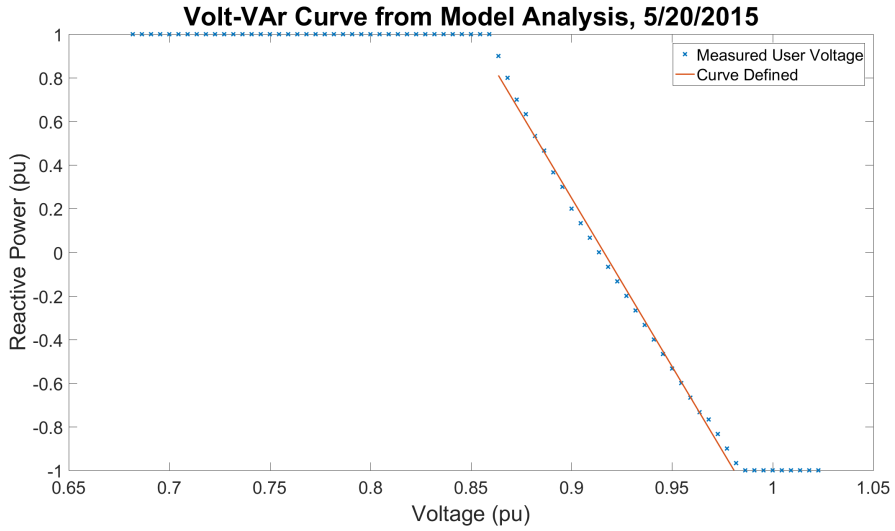

Figure 15: Volt-Var curve as defined by the OpenDSS model, given the optimality conditions seen in Table 2. The slope of the linear fit to the data is the droop factor of this curve.

For the mathematically formulated solution, Table 2 shows the optimality conditions used to develop these volt-var curves.

Table 2: Conditions for volt-var curve formulation the the mathematical and modeled systems. The stabilizing volt-var curves are defined by these parameters

	Mathematical	Actual
Setpoint	200.7 V	200.7 V
Deadband	0	0
Droop Factor	-17.48	-15.57

3.4 Power Flow Simulations

The optimized volt-var curve was implemented to stabilize the voltage at the user. The results of this stabilization are seen in in Figure 16.

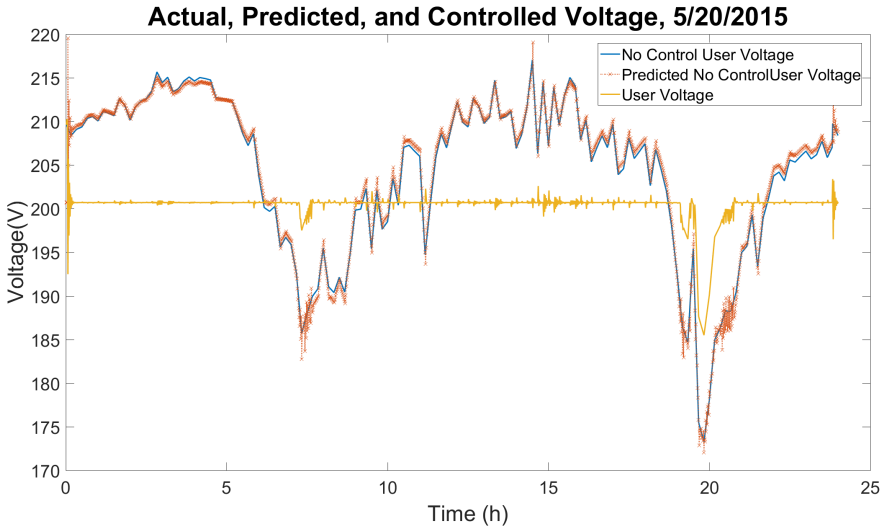

Figure 16: OpenDSS simulation results with predictor and volt-var control.

3.5 Validation

In order to compare the results at varying setpoints, the variance and percentage of voltage violations of the resultant voltage are seen in Table 3. The variance of the original voltage is 80.87 for 5/20/2015, with a nominal voltage of 220V. A voltage perturbation of ± 2 volts was considered to be a voltage violation for this analysis.

Table 3: Variance and voltage violations at specified voltage setpoints. Setpoints were based off of pu values, and the proposed optimization voltage from the mathematical formulation.

Setpoint	187V (.85pu)	200V (.9pu)	200.7V (Math Opt.)	209V (.95pu)	220V (1pu)
Droop Factor	-14.31	-15.57	-15.46	-16.20	-18.43
Variance	17.76	3.33	3.73	7.89	57.32
% Violations	56.94%	5.49%	6.39%	12.71%	50.21%

4 Discussion

The day chosen for analysis was chosen simply because there are no gaps in the data collected, the RIDS-Nepal office did not island from the grid at any point in time, and the measurements taken contain no special events. Figures 6 through 8 show the "regular" nature of the data collected on this day. It is clear that the system is grid connected through out the day, as the voltages measured at the user load and inverters are equivalent throughout the day as represented in Figure 6. Power usage, as is seen in Figure 7 is consistent with that which would be expected. There are spikes in load in the morning, evening, and at night - at times when a homeowner is generally getting ready for work in the morning, returning from work using general household appliances to prepare food or for leisure, using lighting, and again preparing for bed. Consistent throughout the day is also a base load of just under .1 kW. The current of the PV connected inverter, visualized in Figure 8, is consistent with daily irradiance trends, and indicate a generally sunny day with some cloud cover.

Reconstruction of the distribution feeder was integral to this analysis. Keeping the high variability of the voltage at the user was especially important, as the goal of this research was to stabilize the highly variable voltage. Figure 9 shows the user voltage of the collected data and the modeled feeder. The voltages are the same at most times, but do vary occasionally. This is likely due to other dynamics modeled on the feeder, as the differences are similarly correspond with times of increased power flow at other loads the distribution feeder. Figure 10 shows reconstructed feeder conditions, based on the methods outlined in this work. It is clear that the variability of the feeder is conserved. Though not used for any of detailed analysis in this work, this step is important for any future work to be considered with this dataset. It is also important for consistency of results for analysis such as these on longer terms.

Figure 11 shows expected behavior of our predictor algorithm, without any control applied. Since no control is applied, we $\hat{v}(t) = \bar{v}(t)$, and the predictor should track the actual voltage exactly. Since the predictor algorithm assumes linearity from $v(t-1)$ to $\hat{v}(t+1)$ based on linearity with $v(t)$, when the nonlinearities of the signal appear, errors are seen in the prediction. Many researchers discuss the details of nonlinear approximations in prediction algorithms throughout numerous disciplines of study. The purpose of this research was to demonstrate the possibility of reactive power voltage stabilization. As such, the variabilities of different prediction algorithms based on different linearization and approximation techniques is left for future and other research.

The optimization of a Volt-Var curve based on the mathematical formulation provided a

near-optimal solution. Figure 12, shows the variance of the daily simulation given varying voltage deadband widths and voltage setpoints. It is expected that this produce a resultant zero deadband, as adding a deadband to the volt-var curve simply allows for more variance of the system. A voltage setpoint of 200.7 volts that minimized the variance of the model and is shown in Table 2 was used as a baseline for the implementation of a volt-var curve to the OpenDSS model. The violation minimization provided broader results, but also behaved as expected. Minimum numbers of violations were seen near the average of the voltage on the feeder without control action. Also, when the deadband was defined as larger than the given tolerance of 5 volts, the violations increased rapidly as the algorithm was no longer acting to optimize within the tolerance bounds. Considering Figures 14 and 15 and the droop factor's of the optimized volt-var curve, the mathematical and modeled results differ slightly. This is likely a result of the increased complexity of the modeled simulation. The modeled feeder provides nonlinearities and more complex power flow than the mathematical representation suggests, and thus a change in reactive power expectedly has less of an impact on the voltage at any point.

In defining a volt-var curve that optimized to the voltage setpoint found through the mathematical formulation of the system, the voltage stabilization in Figure 16 was found. The predictor was able to track the expected user voltage without control well, thus providing a stabilized voltage. It should be noted that precise tracking by the observer is not as important as the stabilization of the voltage. A poorly predicted voltage that provides a well stabilized voltage is acceptable, while a well predicted voltage that does not lead to a stable voltage is not.

Table 3 shows the final validation of the optimization result on the OpenDSS feeder. Per unit voltage values and the solution proposed by the mathematical result are shown. As is seen, a setpoint of 200V is seen to be slightly more optimal than the mathematical result, considering the optimality conditions suggested in this research. It should be noted that for this formulation, a violation was considered of being ± 2 volts. If the violation tolerance is constrained to ± 1 volt, the 200.7V %violations is reduced to less than that of the 200V solution volts.

5 Summary

This work presents successful formulation of volt-var control curves for long term voltage stabilization on a highly variable distribution feeder. Previous research has investigated the use of smart inverter volt-var curves to stabilize voltages on more stable distribution feeders [9] [6]. By modifying the inverter's condition as an inductive or conductive load, perturbations in voltage can be reduced or removed. Here, we have defined optimization methods for a volt-var curve given known, and highly variable distribution feeder conditions.

Through data collected at the RIDS-Nepal site in Kathmandu, Nepal, the distribution feeder conditions were reconstructed in the open source distribution system simulation software, OpenDSS. Successful parameterization of the feeder lead to the user voltage conditions that are seen in Figure 9, and contain the same characteristics as the measured user voltage. A voltage predictor was then created, as demonstrated in Figure 11, to track the expected voltage of the feeder with and without control. In parallel, volt-var curves were also defined using mathematical models (Equation 8) and distribution feeder models. The optimized voltage setpoint found through the mathematical description of the reactive power - voltage relationship was used to perform initial stability analysis of the feeder with implemented volt-var curves. The results of this analysis are seen in Figure 7 and Table 3. An optimal volt-var curve for the modeled system was found to have a setpoint of approximately 200V with a droop factor of -15.57. This stabilized the voltage to an optimal variance of 3.33, far better than the initial voltage variance of 80.87. This condition also resulted in an $\approx$5% violation rate, when a tolerance of $\pm$2 volts was defined.

There are a number of future developments of this work that would require a larger feeder model to be developed. Successful modeling would be dependent on the ability to take more local feeder measurements. To highlight a few potential next steps for this research, a variety of different approaches to this work could be taken. Rather than simulating a larger %penetration at the RIDS-Nepal site than exists, a larger %penetration could be achieved by simulating more distributed PV dispatch at the RIDS-Nepal site, and neighboring homes. In doing so, the optimality condition of the volt-var curve could be redefined. In this research, we stabilized the voltage at the site in question, but did not concern ourselves with the surrounding area. A different form of optimality could be achieved in stabilizing the neighborhood voltage as much as possible, rather than stabilizing the voltage at one site. This opens the door to many different facets of research, ranging from further definition of what is optimal to coordinated and predictive inverter control, to economic analyses of

the advantages of increased access to stable energy in regions of the world with distribution feeders such as these. This research has presented a solution to small-disturbance, long term voltage instability on distribution feeders with high variability. The work contributes to the potential viability and value distributed energy resources in the developing energy markets of the world by introducing a method of preserving one important aspect of power quality while also increasing general access to energy.

References

[1] "First report of power system stability," *Electrical Engineering*, vol. 56, pp. 261–282, Feb 1937.

[2] P. Kundur, N. Balu, and M. Lauby, *Power system stability and control*. EPRI power system engineering series, McGraw-Hill, 1994.

[3] P. Kundur, J. Paserba, V. Ajjarapu, G. Andersson, A. Bose, C. Canizares, N. Hatziargyriou, D. Hill, A. Stankovic, C. Taylor, T. V. Cutsem, and V. Vittal, "Definition and classification of power system stability ieee/cigre joint task force on stability terms and definitions," *IEEE Transactions on Power Systems*, vol. 19, pp. 1387–1401, Aug 2004.

[4] C. M. Colson and M. H. Nehrir, "A review of challenges to real-time power management of microgrids," in *2009 IEEE Power Energy Society General Meeting*, pp. 1–8, July 2009.

[5] T. V. Cutsem, "Voltage instability: phenomena, countermeasures, and analysis methods," *Proceedings of the IEEE*, vol. 88, pp. 208–227, Feb 2000.

[6] J. W. Smith, W. Sunderman, R. Dugan, and B. Seal, "Smart inverter volt/var control functions for high penetration of pv on distribution systems," pp. 1–6, March 2011.

[7] EPRI OpenDSS, "Open Distribution System Simulator." http://sourceforge.net/projects/electricdss/, 2016.

[8] D. Chianese, D. Pittet, J. Shrestha, D. Sharma, A. Zahnd, M. Upadhyaya, S. Thapa, N. Sanjel, and M. Shah, "Development of pv grid-connected plants in nepal. a feasibility study and training programme co-financed by repic," 2010.

[9] T. Fawzy, D. Premm, B. Bletterie, and A. Goršek, "Active contribution of pv inverters to voltage control – from a smart grid vision to full-scale implementation," *e & i Elektrotechnik und Informationstechnik*, vol. 128, no. 4, pp. 110–115, 2011.

[10] I. M. S. Heslop and J. Fletcher, "Meximum pv generation estimation method for residential low voltage feeders," Apr 2015.